

RESEARCH

Open Access



Synthesis of inventive biphenyl and azabiphenyl derivatives as potential insecticidal agents against the cotton leafworm, *Spodoptera littoralis*

Eslam A. Ghaith^{1*}, Hajar A. Ali¹, Mohamed A. Ismail¹, Abd El-Aziz S. Fouda¹ and M. Abd El Salam²

Abstract

The emergence of pest resistance of *Spodoptera littoralis* (order; Lepidoptera, family; Noctuidae) towards the large scale of different classes of insecticides necessitates the development of some new poly-functionalized biphenyl and azabiphenyl with highly anticipated insecticidal bioresponse. Four new biphenyl carboxamidines **4a–d** and four aza-analogue picolinamidine derivatives **8a–d** were designed and prepared via the treatment of their corresponding carbonitriles with lithium-*bis* trimethylsilylamide [LiN(TMS)₂], followed by hydrolysis with hydrogen chloride. Furthermore, these compounds were elucidated by spectral data, and their toxicity and insecticidal activity were screened against *Spodoptera littoralis*. Whereby, toxicological and biochemical aspects of the inventively synthesized biphenyl and azabiphenyl derivatives against the cotton leafworm, *Spodoptera littoralis* were inspected. As regards the indomitable LC₅₀ and LC₉₀ values, biphenyl and aza-analogues **8d**, **8a**, **4b**, and **8b**, revealed the furthestmost forceful toxic effects with LC₅₀ values of 113.860, 146.265, 216.624, and 289.879 ppm, respectively. Whereby, their LC₉₀ values are 1235.108, 1679.044, 2656.296, and 3381.256 ppm, respectively, and toxicity index being 22.31%, 17.36%, 11.72%, and 8.76%, respectively, comparing with the already recommended, methomyl insecticide, lannate 90% SP (LC₅₀, 25.396 and LC₉₀, 57.860 and toxicity index, 100%). Additionally, electrochemical parameters via DFT studies were carried out for demonstrating and elucidation of structure–activity relationship (SAR) according to highly motivated compounds' descriptors, and the in vivo insecticidal activities.

Keywords Biphenyl, Picolinamidine, *Spodoptera littoralis*, DFT studies

*Correspondence:

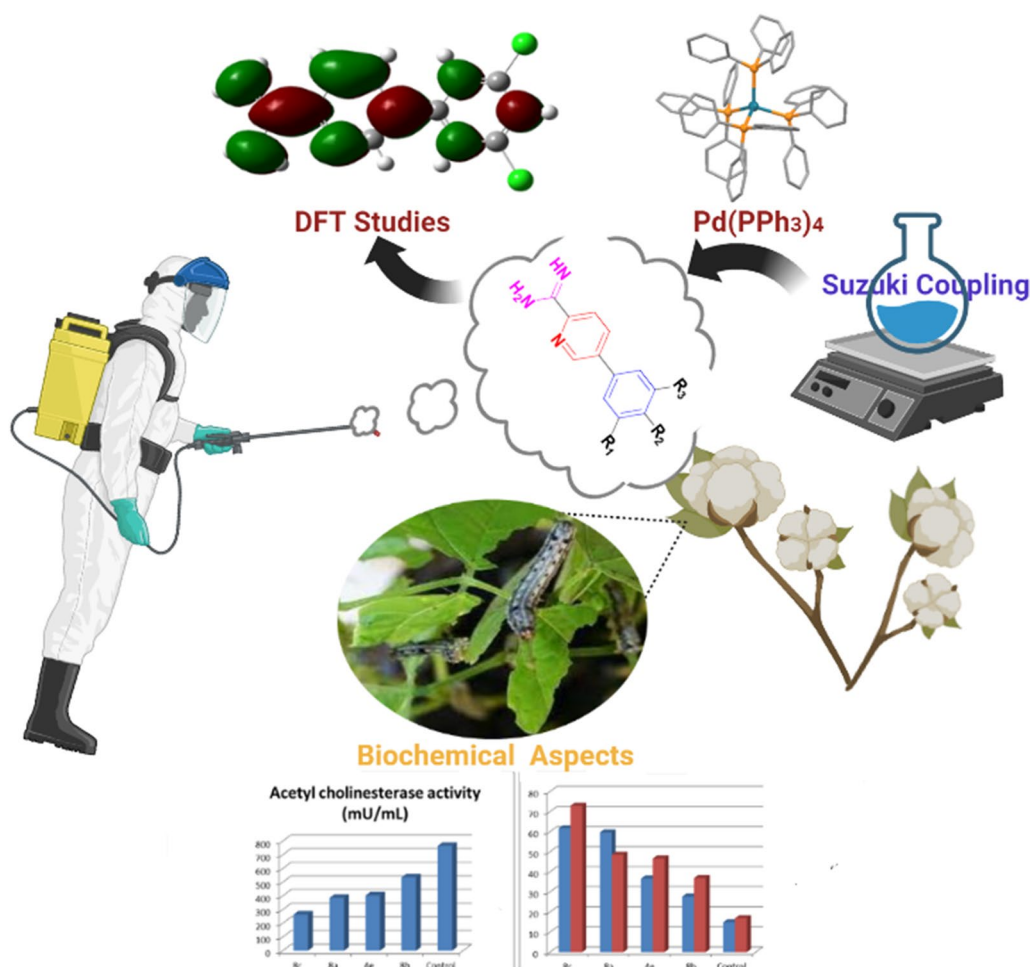
Eslam A. Ghaith
abdelghaffar@mans.edu.eg

Full list of author information is available at the end of the article



© The Author(s) 2023. **Open Access** This article is licensed under a Creative Commons Attribution 4.0 International License, which permits use, sharing, adaptation, distribution and reproduction in any medium or format, as long as you give appropriate credit to the original author(s) and the source, provide a link to the Creative Commons licence, and indicate if changes were made. The images or other third party material in this article are included in the article's Creative Commons licence, unless indicated otherwise in a credit line to the material. If material is not included in the article's Creative Commons licence and your intended use is not permitted by statutory regulation or exceeds the permitted use, you will need to obtain permission directly from the copyright holder. To view a copy of this licence, visit <http://creativecommons.org/licenses/by/4.0/>. The Creative Commons Public Domain Dedication waiver (<http://creativecommons.org/publicdomain/zero/1.0/>) applies to the data made available in this article, unless otherwise stated in a credit line to the data.

Graphical Abstract



Introduction

Every year, harmful insect pests in agriculture cause considerable losses in crops, and productivity around the world [1–3]. As a result of the incidence of pests, especially animal pests, the growth and productivity of crops become at continuous risk. Despite many measures and developments in crop protection, increasing estimates of actual and potential losses according to Food and Agriculture Organization (FAO) are frequently reported [4–6]. One of the major causes is increased pest resistance to insecticides, which has gradually spread and affected crop growth and harvest [7–10]. Over recent decades, the Egyptian cotton leafworm, *Spodoptera littoralis*, Boisduval (Order; Lepidoptera, Family; Noctuidae) has remained one of the most important and dangerous widespread pests affecting cotton and many important

field crops, ornamental plants, vegetables, and weeds in Egypt and many countries over the world [10–12]. As it causes severe damage to these host plants and thus negatively affects the quantity and the quality of agricultural production, subsequently, affecting the national economy of these countries, and increasing the food gap around the world [13–17].

As a result of the increased and excessive use of agricultural pesticides to combat this pest, this led to the emergence of pest resistance, as well as the persistence of residues of these pesticides for long periods, which has adverse effects on humans and beneficial non-target organisms as predators parasites, and thus leads to environmental pollution and disruption of the natural balance [18–20]. For these reasons, we had to build up some inventive bioactive polyfunctionalized biphenyl

isosteres of probable insecticidal effectiveness against *S. littoralis* under laboratory circumstances, that are safer for the environment, and less toxic to mammals, without forming cross-resistance to other insecticides [21].

Likewise, assessment of the action of the ultimate potent investigated insecticides by the assessment of enzymatic activities as biochemical aspects for instance, Alk-p, Acid-P, total lipids, lipase activity, total protein, and amylase activity, ALT, AST, and Ach-E. On the other hand, nitrogenous heterocyclic molecules have been playing a crucial role as fungicides, herbicides, insecticides, and plant growth regulators [22–25]. Additionally, compounds containing phenylpyridine derivatives such as halauxifen-methyl, florpyrauxifen-benzyl and boscalid exhibited excellent biological activity against insecticides, fungicides, and herbicides (Fig. 1) [7, 26]. In the same context, the use of halogenated compounds in the development of agrochemical research has significant expansion in the last decade [27, 28]. Encouraged by the aforementioned results, a series of novel biphenylcarboxamide and their aza-biphenyl analogs substituted with halogens (Cl, F) were designed and synthesized with anticipated pesticidal properties.

Results and discussion

Chemistry

A novel mono cationic biphenyl carboxamide derivatives **4a–d** (Scheme 1) were prepared through subsequent steps. Firstly, Suzuki-Miyaura coupling reaction (SMC) of bromobenzonitrile derivatives with substituted phenylboronic acids **2a–c** in the presence of tetrakis(triphenylphosphine)palladium(0) ($\text{Pd}(\text{PPh}_3)_4$) as a strong electron-donating and sterically bulky catalyst/ligand afforded biphenylnitriles **3a–d** in acceptable yield (69–82%) [29]. Secondly, compounds **3a–d** were converted to the corresponding free bases of biphenyl carboxamides **4a–d**, on treatment with $\text{LiN}(\text{TMS})_2$ followed by hydrolysis with hydrogen chloride/EtOH solution. Then, carboxamide derivatives were neutralized with NaOH to yield the corresponding free bases. Finally, the monoamides hydrochloride salts **4a–d** were synthesized by the reaction of the free base of monoamides with a mixture of hydrogen chloride/EtOH solution. It is worthy to mention that the attempts to achieve the optimum condition for compounds **3a–d** through using different palladium salts palladium(II) carbonate and palladium(II) nitrate ($\text{Pd}(\text{NO}_3)_2$) led to tedious chromatographic purification and did not impart any increase in

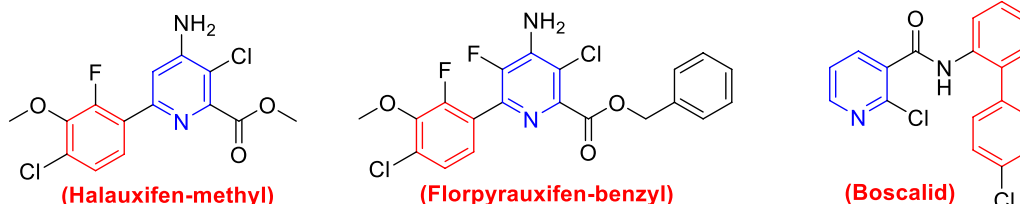
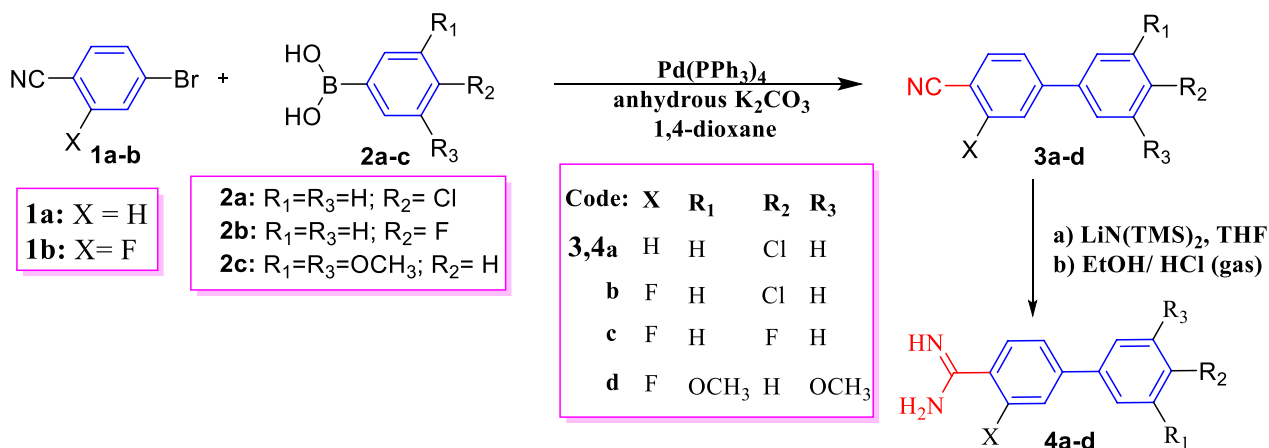


Fig. 1 Biologically active aza-biphenyl derivatives



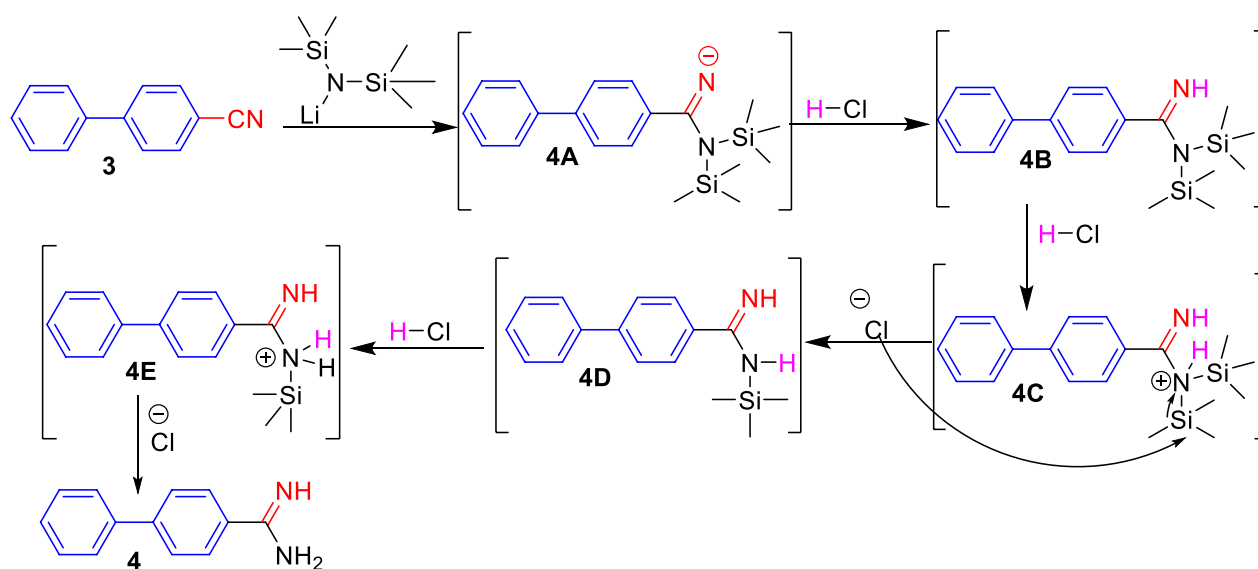
Scheme 1 Synthesis scheme for the new biphenyl carboxamide derivatives **4a–d**

yields (50–56%). The spectral analyses of compounds **3a–d** were in accordance with their suggested structures. As IR spectra of all mononitriles **3a–d** revealed the appearance of the cyano groups in the range of 2225–2231 cm^{-1} . Whereby, mass spectra of compound **3a** gave molecular ion peaks m/z at 213.77 (M^+) and 215.63 ($M^+ + 2$) due to the presence of chlorine isotopes. ^1H -NMR spectrum of the biphenylcarbonitrile derivative **3a** displayed four doublet signals resonated at $\delta = 7.54, 7.75, 7.86$, and 7.91 ppm with coupling constants of $J = 9$ Hz due to four aromatic-H's of benzonitrile ring and four aromatic-H's of *para*-chlorophenyl ring, respectively. While in the case of compound **3b**, the presence of fluorine atom in the benzonitrile ring gave a molecular ion peak m/z at 231.15 and 233.15. Whereas a molecular ion peak for compound **3c** appeared at m/z 215.15. ^1H -NMR spectrum of compound **3d** showed a characteristic singlet signal at $\delta = 3.81$ ppm corresponding to *meta*-dimethoxy-H's. On the other hand, IR spectra of compounds **4a–d** confirmed the disappearance of nitrile groups while arising new amidine protons corresponding to NH_2 , $^+\text{NH}_2$ groups. ^1H -NMR spectrum of compound **4a** confirmed the presence of amidine protons at $\delta = 9.31, 9.52$ ppm and eight aromatic protons; four of them related to *para*-chlorophenyl ring at $\delta = 7.56$ and 7.81 ppm with J coupling constant 6.5 Hz, whereas the other four protons of benzamidine ring appeared as multiplet signals at $\delta = 7.92$ – 7.96 ppm. The ^{13}C -NMR of compound **4a** displayed eight signals corresponding to molecular formula $\text{C}_{13}\text{H}_{11}\text{ClN}_2$, and showed a characteristic signal resonated at $\delta = 165.18$ ppm attributed to amidine carbon as showed in supplementary file. In addition, the mass spectrum for chlorobiphenyl amidine **4a** displayed molecular ion peaks at (M^+ , $M^+ + 2$) = 230.82 and 232.46 (44.03, 9.56; chlorine isotopes). The constitution of compound **4b** was affirmed through ^1H -NMR spectrum which showing two singlet signals corresponding to amidine protons at $\delta = 9.51$ and 9.56 ppm, whereby, the aromatic protons corresponding to *para*-chlorophenyl and fluorobenzamidine resonate at $\delta = 7.58, 7.75$ – 7.80 and 7.83 – 7.88 ppm. Whereas, ^{19}F -NMR revealed a singlet signal at $-\delta 112.57$ ppm related to one fluorine atom. In addition, the mass spectrum of **4b** displayed a molecular ion peak at 248.76 compatible with the proposed structure. In the same context, ^1H -NMR spectrum of compound **4c** demonstrated two multiplet signals of aromatic hydrogens of *para*-fluorophenyl ring at $\delta = 7.33$ – 7.38 and 7.73 – 7.77 ppm, while the other three aromatic protons of fluorobenzamidine ring appeared at $\delta = 7.83$ – 7.88 , besides, the constitute value of singlet signals of cationic amidine protons at $\delta = 9.49$ and 9.55 ppm. Furthermore, its mass spectrum displayed that the molecular ion peak of compound **4c**, compatible with the

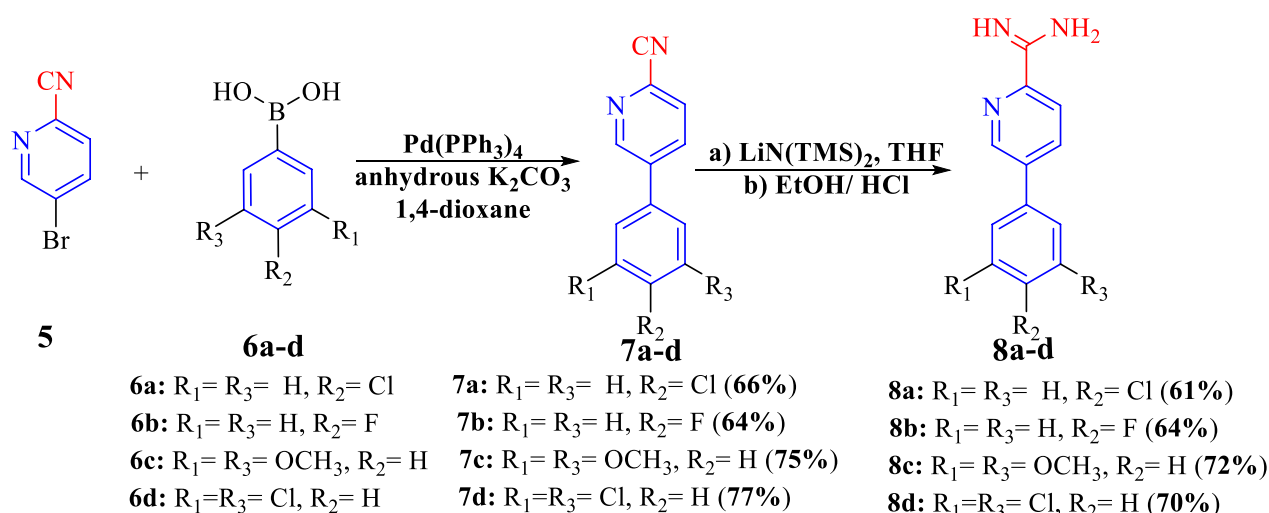
molecular weight at 232.99 corresponding to its molecular formula $\text{C}_{13}\text{H}_{11}\text{F}_2\text{N}_2^+$.

The formation of carboxamidine derivatives **4** may be suggested on the basis of a mechanism that proceeded through the nucleophilic attack of $\text{LiN}(\text{TMS})_2$ to nitrile carbon of biphenylcarbonitrile **3** to furnish [1,1'-biphenyl] (bis(trimethylsilyl)amino)methylene amide **4A** as the mechanism involving the addition of lithium amide to the nitrile group, followed by protonation by desilylation reaction using hydrogen chloride led to the attraction of acidic hydrogen by nitrogenous anion to yield intermediate **4B** [30, 31]. Then, the chloride anion attacks the most positive silicon atom leading to the concurrent expel of trimethylsilyl chloride molecule $(\text{CH}_3)_3\text{SiCl}$ as a volatile liquid. Finally, the previous steps were repeated passing through intermediates **4C** and **4D** till affording carboxamidines **4a–d** (Scheme 2).

On the same manner, treatment of bromopicolinonitrile **5** with substituted-phenylboronic **6a–d** in refluxing dioxane and in the presence of $\text{Pd}(\text{PPh}_3)_4$ and K_2CO_3 yielded the corresponding phenylpicolinonitrile derivatives **7a–d** (Scheme 3). Then, the transformation of phenylpicolinonitriles to phenylpicolinamidine derivatives **8a–d** (Scheme 3) via the same steps mentioned above for synthesis of biphenyl amidine. Spectral analysis of compounds **7a–d** and **8a–d** were in accordance with the suggested structures. The structures of compounds **7a–d** were supported by IR spectra which revealed the presence of nitrile group at 2227 to 2239 cm^{-1} . ^1H -NMR spectrum of compound **7a** manifested two doublet signals at $\delta = 7.61$ and 7.88 ppm with the same $J = 8.4$ Hz for the aromatic protons of the *para*-chlorophenyl ring, another characteristic doublet signal observed at $\delta = 8.13$ ppm with $J = 8.1$ Hz, besides, the presence of doublet of doublet signals at 8.36 and a singlet signal at 9.10 corresponding to Ar-H of picolinonitrile ring. Its ^{13}C -NMR spectrum showed ten signals and exhibited a characteristic signal at $\delta = 117.57$ ppm corresponding to the carbonitrile group. The mass spectrum of picolinonitrile **7a** gave a molecular ion peak for $\text{C}_{12}\text{H}_7\text{ClN}_2$ at $m/z = 214.10$ (M^+ , 85.36%) and 216.15 (27.28%) due to chlorine isotopes. In the ^1H -NMR spectrum of compound **7c**, *meta*-dimethoxy-H's reverberated as a singlet signal at $\delta = 3.83$ ppm and two singlet signals at $\delta = 6.62$ and 6.95 ppm for the Ar-H of dimethoxyphenyl ring. The ^{13}C -NMR spectrum for compound **7c**, revealed eleven carbon signals that corresponded to the elucidated structure and rebounded at $\delta = 55.48$ ppm corresponding to two methoxy groups at meta position and $\delta = 117.65$ ppm for the cyano group. The aromatic protons of picolinonitrile ring were observed as two doublet signals at $\delta = 8.10$ and 8.35 ppm, in addition to a singlet signal that appeared



Scheme 2 The proposed mechanism of the formation of biphenyl carboxamidine **4**



Scheme 3 Synthesis of substituted phenylpicolinamidines

at $\delta=9.10$ ppm. Moreover, its mass spectrum showed a molecular ion peak at m/z 240.20 (100%), for a molecular formula $C_{14}H_{12}N_2O_2$. Conversely, the IR spectra of compounds **8a–d** confirmed that the nitrile group had vanished, while new bands at 3272–3445 that corresponded to NH_2 , $^+NH_2$, and groups had appeared. The 1H -NMR spectrum of compound **8a** exhibited the aromatic protons as two doublet signals at $\delta=7.62$ and 7.92 ppm with $J=9$ Hz for *para*-chlorophenyl ring, while the aromatic protons of picolinamidinium ring reverberated as two doublet and one singlet signals at $\delta=8.44$, 8.50 and 9.14 ppm, respectively. In addition, two singlet signals at 9.46 (s, 2H, H_2N , D_2O exchangeable), and 9.66 ppm (s, 2H,

NH_2^+ , D_2O exchangeable). Whereas, the ^{13}C -NMR spectrum of compound **8a** displayed ten signals and revealed the characteristic carbon signal rebounded at $\delta=161.58$ ppm corresponding to cationic amidinium carbon. Its mass spectrum gave the molecular ion at $m/z=231.0$ and the base peak at $m/z=63.95$. The main characteristic features of 1H -NMR spectrum of **8b** showed two singlet signals at $\delta=9.51$ (s, 2H, NH_2 exchangeable with D_2O), 9.69 ppm (s, 2H, $^+NH_2$ exchangeable with D_2O), in addition two doublet signals related to fluorophenyl at δ 7.40 and 7.96 ppm, whereas, aromatic protons of picolinamidinium appeared as a multiple signals at δ 8.46–8.47 ppm. ^{19}F -NMR showed a characteristic singlet signal at $-\delta$ 112.39

ppm (using TFA as external standard) of fluorine atom. Whereby, its IR spectrum confirmed the disappearance of cyano group while arising a new band at 3411 and 1686 corresponding to NH, C=N, respectively. While, its mass spectrum showed a molecular ion peak at 215.05 which is completely compatible with its molecular weight $C_{12}H_{10}FN_3$. Furthermore, 1H -NMR spectrum for compound **8c** exhibited a characteristic singlet signal at δ 3.83 assigned to two *methoxy groups*, as well as, two singlets at 6.63 and 6.99 ppm for the aromatic protons of dimethoxyphenyl ring. Aromatic protons of picolinamidine ring were found as two doublets at δ =8.42, 9.13 ppm and one doublet of doublet signal at 8.48 with J =1.5 and 8 Hz, besides, two singlet signals at δ =9.45 and 9.65 ppm for amidic protons (H_2N , NH_2^+). A molecular ion peak of compound **8c** was noticed as m/z =257.10 (M^+ , 39.08%) and while m/z =241.05 corresponding to its base peak. Also, ^{13}C -NMR spectrum assured the presence of eleven signals, whereas, amidine carbon resonated at δ =161.61 ppm and two methoxy carbons resonated at 55.50 ppm.

Insecticidal activity

Toxicological activity

Toxicity test for Cotton leaf worm (S. littoralis, Order; Lepidoptera, Family; Noctuidae) The represented data in Table 1 demonstrated the insecticidal efficacy of eight innovatively tested compounds against the 2nd instar larvae of the laboratory strain of the polyphagous pest, cotton leafworm, *S. littoralis* (Boisd.) at different concentrations. The represented data displayed that the mortality percentages directly increase with the increasing of concentrations and days post-treatment. Consequently, compounds; **8d**, **8a**, **4b**, and **8b** were the most potent compounds, where, the mortality percentages of the treated larvae of *S. littoralis* reached 86.67%, 83.34%, 76.67% and 70.00%, respectively. The total of inspected compounds displayed powerful toxic effects after 7 days (based on LC_{50} value). Amongst all, compounds **8d**, **8a**, **4b** and **8b** exhibit excellent results with LC_{50} 's values 113.860, 146.265, 216.624 and 289.879 ppm, respectively. In the same context, the toxicity indexes are 22.31%, 17.36%, 11.72%, and 8.76%, respectively, compared with the already recommended, methomyl insecticide, lannate 90% SP (LC_{50} , 25.396 & LC_{90} , 57.860 and toxicity index, 100%), according to the toxicity data denoted in Table 2.

Biochemical impacts

A. Alkaline phosphatase (Alk-P) and Acid phosphatase (Acid-p) analyses In Table 3, the data presented that **8d** achieved the highest drop in the activity of Alk-P, lower than in the control, it was – 41.99%, followed by **8a**, **4b**, of which, it was by – 35.81, – 30.63%, respectively, while the nethermost decrease in Alk-P activity was prompted by

Table 1 Mortality% of the 2nd instar larvae of cotton leafworm, *S. littoralis* after treatment by the newly synthesized compounds compared with Methomyl insecticide, Lannate 90% SP after 7 days of treatment

Tested compounds	Concentrations	Mortality % after days post treatment			
		1 day	3 days	5 days	7 days
Lannate 90% SP	12.5	3.33	6.67	10.00	13.33
	25	26.67	30	36.67	46.67
	50	66.67	76.67	83.33	90
	100	80.00	83.33	90.00	96.67
8d	25	3.34	10.00	16.67	20.00
	50	6.67	13.34	20.00	30.00
	100	23.34	33.34	43.34	53.34
	200	30.00	40.00	53.34	63.34
	400	33.34	43.34	56.67	70.00
	800	46.67	63.34	76.67	86.67
8a	25	0	3.34	10.00	16.67
	50	0	6.67	16.67	26.67
	100	16.67	26.67	36.67	46.67
	200	23.34	36.67	46.67	60.00
	400	26.67	40.00	53.34	63.34
	800	50.00	60.00	73.34	83.34
4b	25	0	0	6.67	10.00
	50	0	3.34	13.34	23.34
	100	13.34	23.34	36.67	43.34
	200	16.67	26.67	40.00	50.00
	400	23.34	33.34	43.34	53.34
	800	46.67	56.67	66.67	76.67
8b	25	0	0	0	6.67
	50	0	0	6.67	16.67
	100	6.67	16.67	26.67	36.67
	200	13.34	23.34	33.34	43.34
	400	16.67	26.67	40.00	50.00
	800	36.67	46.67	56.67	70.00
4c	25	0	0	0	3.34
	50	0	0	3.34	13.34
	100	3.34	6.67	20.00	30.00
	200	6.67	16.67	26.67	36.67
	400	13.34	23.34	36.67	46.67
	800	33.34	43.34	53.34	63.34
4a	25	0	0	0	0
	50	0	0	0	6.67
	100	0	3.34	13.34	23.34
	200	6.67	13.34	20.00	33.34
	400	3.34	13.34	23.34	36.67
	800	13.34	26.67	43.34	53.34
4d	25	0	0	0	0

Table 1 (continued)

Tested compounds	Concentrations	Mortality % after days post treatment			
		1 day	3 days	5 days	7 days
8c	50	0	0	0	0
	100	0	0	3.34	13.34
	200	0	0	6.67	20.00
	400	3.34	6.67	20.00	30.00
	800	6.67	23.34	33.34	43.34
	25	0	0	0	0
	50	0	0	0	0
	100	0	0	0	6.67
	200	0	0	3.34	13.34
	400	0	3.34	10.00	16.67
	800	3.34	16.67	26.67	36.67

Bold represents the optimal concentration exhibiting the highest efficacy of each tested compound as an insecticidal agent after 7 days post treatment

8b, by – 26.82% lower than the control sample. Additionally, **8d** revealed the maximum reduction in the activity of Acid-P lower than in the control, it was – 85.10%, followed by **8a**, **4b**, of which, it was by – 81.94, – 78.84%, whereas **8b** caused the lowest drop in Acid-P activity, by – 73.96% less than the control sample.

B. Total proteins and total lipids activity's analyses Looking at Table 4, it can be detected that all of the examined compounds produced a reduction in total proteins; it ranged from – 3.96 to – 73.97% lower than in the control. The activity of the **8d** treated with larvae reached to its lowest level (– 85.07% lower than in the control), and **8b** caused the least salient decrease in the total lipids' activity (– 2.86% compared to the control). The results showed that all of the synthesized compounds tested caused a notable reduction in total lipid activity (Table 4).

C. Determination of lipase and amylase activity Table 5 depicts the results of lipase and amylase activities for the tested compounds, as compound **8d**

Table 2 Toxicity bioresponses of the recently synthesized compounds towards the 2nd instar larvae of cotton leafworm, *S. littoralis* compared with methomyl insecticide, Lannate 90% SP after 7 days post treatment

Tested compounds	LC ₅₀ (ppm) and confidence limits at 95%	LC ₉₀ (ppm) and confidence limits at 95%	Slope	Toxicity index % at LC ₅₀ value	Relative potency
Lannate 90% SP	25.396	57.860	3.584 ± 0.552	100	74.47
	20.725	45.600			
	30.600	85.143			
8d	113.860	1235.108	1.238 ± 0.207	22.31	16.61
	75.479	653.341			
	165.348	3990.189			
8a	146.265	1679.044	1.209 ± 0.205	17.36	12.93
	98.758	836.464			
	217.972	6226.086			
4b	216.624	2656.296	1.177 ± 0.206	11.72	8.73
	147.368	1198.720			
	346.844	12500.646			
8b	289.879	3381.256	1.201 ± 0.211	8.76	6.53
	197.005	1467.575			
	492.252	17390.008			
4c	400.239	4369.241	1.235 ± 0.220	6.35	4.73
	267.559	1811.834			
	739.401	25266.588			
4a	666.646	9419.460	1.114 ± 0.209	3.81	2.84
	437.575	3615.027			
	1249.568	68880.669			
4d	1048.448	12951.331	1.174 ± 0.208	2.42	1.81
	710.313	5598.709			
	1758.127	67818.313			
8c	1891.266	20255.647	1.245 ± 0.180	1.34	1.00
	1320.721	9886.043			
	2980.333	68954.267			

Toxicity index is demarcated as the ratio of the utmost operative compound's LC₅₀ value to the other examined compound's LC₅₀ value multiplying by 100

Table 3 The activities of Alk-P and Acid-p in Hemolymph of the 4th Instar Larvae of *S. littoralis* later 5 days of action with LC₅₀ of **8d**, **8a**, **4b**, and **8b** tested compounds

Tested compounds	Alkaline phosphatase (U/L)	% of control	Acid phosphatase (U/L)	% of control
8d	56.45 ± 0.28 ^e	– 41.99	18.37 ± 0.23 ^e	– 85.10
8a	62.47 ± 0.22 ^d	– 35.81	22.26 ± 0.27 ^d	– 81.94
4b	67.51 ± 0.23 ^c	– 30.63	26.08 ± 0.28 ^d	– 78.84
8b	71.22 ± 0.27 ^b	– 26.82	32.10 ± 0.44 ^b	– 73.96
Control	97.31 ± 0.22 ^a		123.23 ± 0.40 ^a	

Whereby, means ± SE (standard error) of 3 replicates of 50 of 4th larvae each. Distinct letters designate significant variances between treatments as stated by Duncan's test. LSD = 0.05 was 0.769 U/L for **Alk-P** and 1.048 U/L for **Acid-p**. % of control = (test–control)/control × 100

Table 4 Total proteins and total lipids, activities in the hemolymph of the 4th Instar Larvae of *S. littoralis* later 5 days of treatment with LC₅₀ of **8d**, **8a**, **4b**, and **8b** tested compounds

Tested compounds	Total proteins (g/dL)	% of control	Total lipids (g/dL)	% of control
8d	5.40 ± 0.31 ^d	– 73.97	3.03 ± 0.12 ^d	– 85.07
8a	8.19 ± 0.27 ^c	– 60.52	8.36 ± 0.30 ^c	– 58.82
4b	14.40 ± 0.31 ^b	– 30.57	14.63 ± 0.35 ^b	– 27.93
8b	19.92 ± 0.20 ^a	– 3.96	19.72 ± 0.35 ^a	– 2.86
Control	20.74 ± 0.31 ^a		20.30 ± 0.28 ^a	

Whereby, means ± SE (standard error) of 3 replicates of 50 of 4th larvae each. Distinct letters designate significant variances between treatments as stated by Duncan's test. LSD = 0.05 was 0.888 g/dL for total proteins and 0.921 g/dL for total lipids. % of control = (test–control)/control × 100

Table 5 Lipase and amylase activities in Hemolymph of the 4th Instar Larvae of *S. littoralis* after 5 days of exposure with LC₅₀ of **8d**, **8a**, **4b**, and **8b** tested compounds

Tested compounds	Lipase activity (U/mL)	% of control	Amylase activity (U/mL)	% of control
8d	0.121 ± 0.004 ^a	47.56	0.098 ± 0.002 ^b	– 56.06
8a	0.024 ± 0.007 ^c	– 70.73	0.078 ± 0.007 ^b	– 65.03
4b	0.024 ± 0.002 ^c	– 70.73	0.041 ± 0.002 ^c	– 81.62
8b	0.038 ± 0.002 ^c	– 53.66	0.024 ± 0.003 ^c	– 89.24
Control	0.082 ± 0.002 ^b		0.223 ± 0.015 ^a	

Whereby, means ± SE (standard error) of 3 replicates of 50 of 4th larvae each. Distinct letters designate significant variances between treatments as stated by Duncan's test. LSD = 0.05 was 0.038 U/mL for lipase and 0.023 U/mL for amylase. % of control = (test–control)/control × 100

caused a significant increase in the lipase activity; it was 47.56% higher than in the control while the other tested compounds **8a**, **4b**, and **8b** showed a significant decrease in lipase activity; it was by – 70.73, – 70.73 and – 53.66%, respectively, lower than in the control but not significant between each other. Conversely, the obtained results demonstrated that all the investigated compounds caused a notable decrease in the amylase activity (Table 5), the activity of **8b** treated larvae fluctuated to its lowest pattern level (– 89.24% lower than in the control), while **8d**, **8a** and **4b** caused remarkable decrease by – 56.06, 65.03 and 81.62%, respectively, lower than in the control.

D. Alanine aminotransferase (ALT) and aspartate aminotransferase (AST) activities, analyses The data showed that all the established compounds displayed a noteworthy accretion in ALT activity (Table 6), and the enzyme activity reached its ultimate value in **8d** treated larvae (313.18%). Whereas the enzyme activity was observed to be at the lowermost increase in **8b** treated larvae (85.09%). Compounds **8a** and **4b** have remarkable increases in enzyme activity by 299.00% and 145.56%, respectively, higher than the control. In addition, there was a rise in the activity of aspartate aminotransferase (AST) (Table 6). Whereas, compound **8d** was the highest potent compound having insecticidal properties, as it displayed a vastly significant

Table 6 Changes of ALT and AST activities in Hemolymph of the 4th Instar Larvae of *S. littoralis* later 5 days of treatment with LC₅₀ of **8d**, **8a**, **4b**, and **8b** tested compounds

Tested compounds	ALT activity (U/L)	% of control	AST activity (U/L)	% of control
8d	61.77 ± 0.32 ^a	313.18	72.93 ± 0.53 ^a	330.78
8a	59.65 ± 0.47 ^b	299.00	48.60 ± 0.49 ^b	187.07
4b	36.71 ± 0.36 ^c	145.56	46.65 ± 0.28 ^d	175.55
8b	27.67 ± 0.54 ^d	85.09	36.93 ± 0.38 ^c	118.14
Control	14.95 ± 0.70 ^e		16.93 ± 0.54 ^b	

Whereby, means ± SE (standard error) of 3 replicates of 50 of 4th larvae each. Distinct letters designate significant variances between treatments as stated by Duncan's test. LSD=0.05 was 1.341 U/L for ALT and was 1.435 U/L for AST. % of control = (test–control)/control × 100

Table 7 A-chE activity of A-chE in Hemolymph of the 4th Instar Larvae of *S. littoralis* later 5 days of treatment with LC₅₀ of **8d**, **8a**, **4b**, and **8b** tested compounds

Tested compounds	Acetyl cholinesterase activity (mU/mL)	% of control
8d	264.11 ± 0.76 ^e	– 65.50
8a	385.81 ± 0.86 ^d	– 49.61
4b	403.90 ± 1.06 ^c	– 47.24
8b	536.19 ± 1.30 ^b	– 29.96
Control	765.53 ± 1.63 ^a	

Whereby, means ± SE (standard error) of 3 replicates of 50 of 4th larvae each. Distinct letters designate significant variances between treatments as stated by Duncan's test. LSD=0.05 was 3.663 mU/mL for acetyl cholinesterase. % of control = (test–control)/control × 100

enzyme activity exceeding the control sample (330.78%), followed by **8a** (187.07), **4b** (175.55%) then **8b** (118.14%).

E. Acetyl cholinesterase enzyme activity analysis Compound **8d** produced a significant highest reduction in the activity of acetyl cholinesterase activity (A-chE) lower than in the control, it was – 65.50%, followed by **8a** (– 49.61%) and **4b** (– 47.24%) lower than in the control test (Table 7). Whereas, the lowest decrease in A-chE activity was induced by **8b** (– 29.96%) compared to the control test.

Theoretical approaches

Computational calculations were performed using Gaussian 09 program, in the gaseous state, the DFT approach B3LYP as function and 6-311G (d,p) as basis set to investigate chemical reactivity and stability of the geometry optimization preliminary results of expected biological evaluation of the synthesized compounds via studying of different electrochemical parameters such as total energies, spatial distribution of HOMO and LUMO orbitals, energy gap, hardness (η) and global softness (S),

which are depicted in Fig. 2, were carried out through using consequent Eqs. (1, 2, 3, 4) [32–35].

$$\Delta E = (E_{HOMO} - E_{LUMO}) \quad (1)$$

$$\eta = \frac{1}{2}(E_{HOMO} - E_{LUMO}) \quad (2)$$

$$S = \frac{1}{2}\eta \quad (3)$$

$$\mu = \frac{1}{2}(E_{HOMO} + E_{LUMO}) \quad (4)$$

The obtained results showed that highly active compounds in order **8d**, **8a**, **4b**, and **8b** having high softness values than other tested compounds. As global chemical reactivity descriptors such as the energy gap, softness, and chemical potential values, are critical theoretical tools for clarifying the chemical reactivity of the synthesized compounds and the biological activity is directly proportional to increasing with their values. Whereby, a molecule that has a high softness and chemical potential values, is called a soft molecule. Soft molecules are more reactive than hard molecules as they have the ability to donate electrons more easily to acceptors than other molecules. Besides, biological activity depends mainly on the ability of the molecule to offer electrons easily to the acceptor. As seen in the highly potent compounds **8d**, **8a**, **4b**, and **8b**, there are slight differences in their band gaps, softness, and chemical potential values (Fig. 2). [36, 37]. Additionally, the tested molecules display noticeable chemical reactivity descriptors that facilitate prolonged interactions with the enzymes of cotton leafworms. Subsequently, robust disorders in their biochemical and metabolic processes will be carried out, leading to decrease leafworms, growth rates or reduce in their productivity or cause the death of the targeted worms collectively, according to the above-mentioned results.

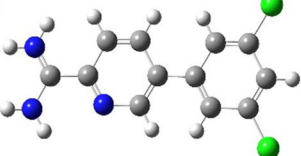
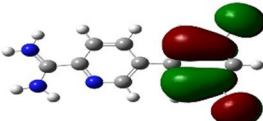
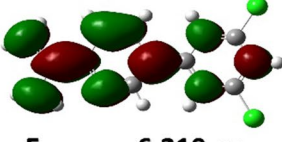
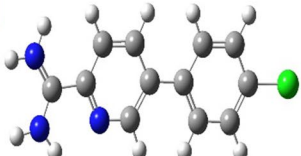
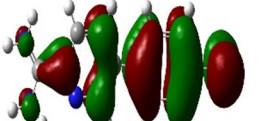
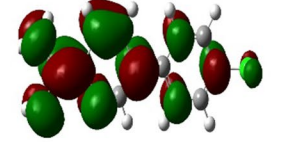
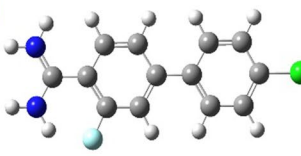


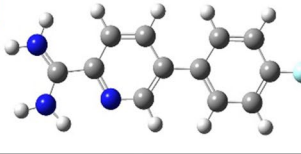
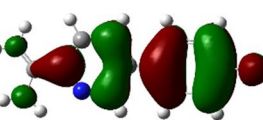
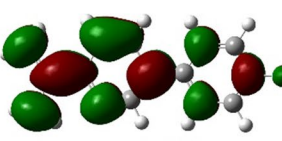
3D	HOMO	LUMO	Electrochemical parameters (E_{gap}), (S), (η), (μ),
8d 	 $E_{\text{HOMO}} = -9.522 \text{ eV}$	 $E_{\text{LUMO}} = -6.210 \text{ eV}$	$E_{\text{gap}} = -3.312 \text{ eV}$ $S = -0.828 \text{ eV}$ $\eta = -1.656 \text{ eV}$ $\mu = -7.866 \text{ eV}$
8a 	 $E_{\text{HOMO}} = -9.277 \text{ eV}$	 $E_{\text{LUMO}} = -6.036 \text{ eV}$	$E_{\text{gap}} = -3.241 \text{ eV}$ $S = -0.810 \text{ eV}$ $\eta = -1.620 \text{ eV}$ $\mu = -7.656 \text{ eV}$
4b 	 $E_{\text{HOMO}} = -9.260 \text{ eV}$	 $E_{\text{LUMO}} = -5.968 \text{ eV}$	$E_{\text{gap}} = -3.292 \text{ eV}$ $S = -0.823 \text{ eV}$ $\eta = -1.646 \text{ eV}$ $\mu = -7.614 \text{ eV}$
8b 	 $E_{\text{HOMO}} = -9.345 \text{ eV}$	 $E_{\text{LUMO}} = -5.983 \text{ eV}$	$E_{\text{gap}} = -3.362 \text{ eV}$ $S = -0.840 \text{ eV}$ $\eta = -1.681 \text{ eV}$ $\mu = -7.664 \text{ eV}$

Fig. 2 The optimized geometrical structures, spatial distribution of calculated HOMO, LUMO orbitals, and global chemical reactivity descriptors of highly potential tested compounds **8d**, **8a**, **4b** and **8b**

Structure activity relationship (SAR)

The main reason for the higher potency of compound **8d** than other test molecules might be rationalized due to the presence of pyridine, amidine moieties, and di-substitution of chloro-atoms enhanced the insecticidal activity [38]. Whereas, the other compounds **8a**, and **8b** containing only one halogenated atom. Whereas, there has been a rise in the number of commercial products containing ‘mixed’ different halogens [28]; in order to explore the essential moiety in insecticidal activity of the synthesized series and aim to investigate the insecticidal activity of molecules that has a mixed or different halogenated atoms chlorine and fluorine atoms we synthesized parent disubstituted halogenated biphenyl compound **4b**. However, compound **4b** showed lower insecticidal potency than compounds **8d** and **8a**; and the addition of different halogens did not impart any benefits; this postulate proves that the most essential active moieties in the synthesized compounds are pyridine and amidine moieties.

Experimental

Chemistry

All devices, equipment, materials, and methods are shown and discussed in detail in the ESI.

General methodology of Suzuki coupling methodology for the preparation of biphenyl carbonitriles **3a-d** was carried out according to the described method [39]

4'-Chloro-[1,1'-biphenyl]-4-carbonitrile (3a**)** A pale-yellow solid; yield = 69%, m.p. = 126.5–128 °C, Lit. [40] m.p. = 125–127 °C, Lit. [41] m.p. = 129–130 °C; R_f = 0.81, EtOAc/petroleum ether (60–80 °C) (1:4). IR (KBr, ν /cm⁻¹): 3067, 3035 (sp² C–H), 2225 (CN), 1604, 1522, 1481 (C=C). ¹H-NMR; δ 7.54 (d, J = 9 Hz, 2H, Ar–H of *para*-chlorophenyl), 7.75 (d, J = 9 Hz, 2H, Ar–H of benzonitrile), 7.86 (d, J = 9 Hz, 2H, Ar–H of benzonitrile), 7.91 ppm (d, J = 9 Hz, 2H, Ar–H of *para*-chlorophenyl). MS (EI) (m/e , %) for C₁₃H₈ClN; 213.77, 215.63 (M^+ , 51.71, 16.19%; chlorine isotopes), 120.09 (Base peak, 100%).

4'-Chloro-3-fluoro-[1,1'-biphenyl]-4-carbonitrile (3b) An off-white solid; yield=70%; m.p.=174–175 °C, Lit. [42] m.p.=175–177 °C; R_f =0.88, EtOAc/petroleum ether (60–80 °C) (1:4). IR (KBr, ν/cm^{-1}): 3086 (sp^2 C–H), 2231 (CN), 1618, 1554, 1482 (C=C). MS (EI) (m/e, %) for $\text{C}_{13}\text{H}_7\text{ClFN}$; 231.15, 233.15 (M^+ , 80.32, 27.18%; chlorine isotopes), 75 (Base peak, 100%).

3,4'-Difluoro-[1,1'-biphenyl]-4-carbonitrile (3c) A white solid; yield=73%; m.p.=118–119 °C. Lit. [43]; R_f =0.91, EtOAc/petroleum ether (60–80 °C) (1:4). IR (KBr, ν/cm^{-1}): 3096, 3069 (sp^2 C–H), 2231 (CN), 1617, 1596, 1560 (C=C). ^1H -NMR; δ 7.33–7.36 (m, 2H, Ar–H of *para*-fluorophenyl), 7.73 (d, J =8.0 Hz, 1H, Ar–H of benzonitrile), 7.85–7.90 ppm (m, 3H), 7.97–8.00 (m, 1H, Ar–H of benzonitrile). MS (EI) (m/e, %) for $\text{C}_{13}\text{H}_7\text{F}_2\text{N}$; 215.15 (M^+ , Base peak, 100%).

3-Fluoro-3',5'-dimethoxy-[1,1'-biphenyl]-4-carbonitrile (3d) A pale-yellow solid yield; 82%, m.p.=114–115 °C; R_f =0.82, EtOAc/petroleum ether (60–80 °C) (1:4). IR (KBr, ν/cm^{-1}): 2953, 2847 (sp^3 C–H), 2230 (CN), 1602, 1561 (C=C). ^1H -NMR; δ 3.81 (s, 6H, *meta*-dimethoxy-H's), 6.59 (s, 1H, Ar–H of dimethoxyphenyl), 6.91 (s, 2H, Ar–H of dimethoxyphenyl), 7.76 (dd, J =8, 1.5 Hz, 1H, Ar–H of fluorobenzonitrile), 7.92 (d, J =1.5 Hz, 1H, Ar–H of fluorobenzonitrile), 7.96–7.99 ppm (m, 1H, Ar–H of fluorobenzonitrile). MS (EI) (m/e, %) for $\text{C}_{15}\text{H}_{12}\text{FNO}_2$; 257.25 (M^+ , Base peak, 100%).

Preparation methodology for biphenylcarboxamidine derivatives 4a–d

Biphenylcarbonitrile derivatives **3a–d** (1.5 mmol) were allowed to react with $\text{LiN}(\text{TMS})_2$ (1M solution in THF, 8 mL, 8 mmol) at room temperature with stirring overnight. After that, ethanol-HCl (gas) solution (12 mL, 1.25 M) was added and the reaction mixture was stirred for another 6 h. The resulting mixture was diluted with diethyl ether (Et_2O) and the formed solid was filtered off. Then, the resultant biphenylcarboxamidine derivative was neutralized with NaOH (1N) and the formed monoamidine-free base was collected, washed with water. Finally, the target biphenylcarboxamidines hydrochloride salts **4a–d** were made from their corresponding free bases on treatment with ethanolic-HCl(gas) solution for overnight, the solid formed was filtered off after addition of Et_2O .

4'-Chloro-[1,1'-biphenyl]-4-carboxamidine hydrochloride salt (4a) An off white solid; yield=74%; m.p.=282–284 °C. IR (KBr, ν/cm^{-1}): 3232 (NH), 3057 (sp^2 C–H), 1720, 1670, 1608, 1540 (C=N & C=C). ^1H -NMR; δ 7.56 (d, J =6.5 Hz, 2H, Ar–H of *para*-chlorophenyl),

7.81 (d, J =6.5 Hz, 2H, Ar–H of *para*-chlorophenyl), 7.92–7.96 (m, 4H, Ar–H of benzamidine), 9.31 (s, 2H, NH_2 exchangeable with D_2O), 9.52 ppm (s, 2H, $^+\text{NH}_2$ exchangeable with D_2O). ^{13}C -NMR; δ 127.01 (1C), 127.05 (2C), 128.94 (4C), 129.18 (2C), 133.69 (1C), 137.17 (1C), 143.85 (1C), 165.18 (1C). MS (EI) (m/e, %) for $\text{C}_{13}\text{H}_{11}\text{ClN}_2$; 230.82, 232.46 (M^+ , 44.03, 9.56%; chlorine isotopes), 219.17 (Base peak, 100%).

4-Chloro-3-fluoro-[1,1'-biphenyl]-4-carboxamidine hydrochloride salt (4b) An off white solid; yield=77%; m.p.=284–286 °C. IR (KBr, ν/cm^{-1}): 3166 (NH), 1673, 1623, 1540 (C=N & C=C). ^1H -NMR; δ 7.58 (d, J =8.0 Hz, 2H, Ar–H of *para*-chlorophenyl), 7.75–7.80 (m, 2H, Ar–H of fluorobenzamidine), 7.83–7.88 (m, 3H, Ar–H), 9.51 (s, 2H, NH_2 exchangeable with D_2O), 9.56 ppm (s, 2H, $^+\text{NH}_2$ exchangeable with D_2O). ^{19}F -NMR ($\text{DMSO}-d_6$); $-\delta$ 112.57 ppm (using TFA as external standard). MS (EI) (m/e, %) for $\text{C}_{13}\text{H}_{10}\text{ClFN}_2$; 248.76 (M^+ , 14.95%), 250.35 ($\text{M}^+ + 2$, 8.23%), 43.22 (Base peak, 100%).

3,4'-Difluoro-[1,1'-biphenyl]-4-carboxamidine hydrochloride salt (4c) An off white solid; yield=74%; m.p.=282–284 °C. IR (KBr, ν/cm^{-1}): 3250 (NH), 3060 (sp^2 C–H), 1680, 1629, 1546 (C=N & C=C). ^1H -NMR; δ 7.33–7.38 (m, 2H, Ar–H of *para*-fluorophenyl), 7.73–7.77 (m, 2H, Ar–H of *para*-fluorophenyl), 7.83–7.88 (m, 3H, Ar–H of fluorobenzamidine), 9.49 (s, 2H, NH_2 exchangeable with D_2O), 9.55 ppm (s, 2H, $^+\text{NH}_2$ exchangeable with D_2O). MS (EI) (m/e, %) for $\text{C}_{13}\text{H}_{10}\text{F}_2\text{N}_2$; 232.99 (M^+ , 84.42%), 119.53 (Base peak, 100%).

3-Fluoro-3',5'-dimethoxy-[1,1'-biphenyl]-4-carboxamidine hydrochloride salt (4d) An off white solid; yield=79%; m.p.=226–228 °C. IR (KBr, ν/cm^{-1}): 3381, 3245 (2NH_2), 3001 (sp^2 C–H), 2841 (sp^3 C–H), 1675, 1598, 1460 (C=N & C=C). ^1H -NMR; δ 3.81 (s, 6H, *meta*-dimethoxy-H's), 6.59 (s, 1H, Ar–H of dimethoxyphenyl), 6.91 (s, 2H, Ar–H of dimethoxyphenyl), 7.73–7.78 (m, 2H, Ar–H of fluorobenzamidine), 7.85–7.88 (d, 1H, J =10.5 Ar–H of fluorobenzamidine), 9.49 (s, 2H, NH_2 exchangeable with D_2O), 9.55 ppm (s, 2H, $^+\text{NH}_2$ exchangeable with D_2O). MS (EI) (m/e, %) $\text{C}_{15}\text{H}_{15}\text{FN}_2\text{O}_2$; 274.95 (M^+ , 47.95%), 167.89 (Base peak, 100%).

General methodology for the preparation of picolinonitrile derivatives 7a–d

Picolinonitrile derivatives **7a–d** were prepared to adopt the same Suzuki coupling conditions used for the synthesis of biphenyl carbonitriles **3a–d**, starting with 5-bromopicolinonitrile and the appropriate phenylboronic acid.

5-(4-Chlorophenyl)picolinonitrile (7a) A yellow solid; yield = 66%; m.p. = 144–145 °C; R_f = 0.84, EtOAc/petroleum ether (60–80 °C) (1:4). IR (KBr, ν/cm^{-1}): 3055 (sp^2 C–H), 2228 (CN), 1653, 1595, 1499 (C=N & C=C). ^1H -NMR; δ 7.61 (d, J = 8.4 Hz, 2H, Ar–H of *para*-chlorophenyl), 7.88 (d, J = 8.4 Hz, 2H, Ar–H of *para*-chlorophenyl), 8.13 (d, J = 8.1 Hz, 1H, Ar–H of picolinonitrile), 8.36 (dd, J = 8.1, 2.4 Hz, 1H, Ar–H of picolinonitrile), 9.10 ppm (s, 1H, Ar–H of picolinonitrile). ^{13}C -NMR; δ 117.57 (1C), 129.10 (2C), 129.21 (2C), 129.29 (1C), 131.40 (1C), 134.07 (1C), 134.46 (1C), 135.40 (1C), 137.70 (1C), 149.22 (1C). MS (EI) (m/e, %) for $\text{C}_{12}\text{H}_7\text{ClN}_2$; 214.10, 216.15 (M^+ , 85.36, 27.28%; chlorine isotopes), 75.10 (Base peak, 100%).

5-(4-Fluorophenyl)picolinonitrile (7b) A white solid; yield = 64%; m.p. = 146–147 °C, Lit. [44]; R_f = 0.84, EtOAc/petroleum ether (60–80 °C) (1:4). IR (KBr, ν/cm^{-1}): 3066 (sp^2 C–H), 2231 (CN), 1605, 1561, 1515 (C=N & C=C). ^1H -NMR; δ 7.36–7.42 (m, 2H, Ar–H of *para*-fluorophenyl), 7.88–7.92 (m, 2H, Ar–H of *para*-fluorophenyl), 8.12 (d, J = 8.1 Hz, 1H, Ar–H of picolinonitrile), 8.34 (dd, J = 8.1, 1.5 Hz, 1H, Ar–H of picolinonitrile), 9.09 ppm (s, 1H, Ar–H of picolinonitrile). MS (EI) (m/e, %) for $\text{C}_{12}\text{H}_7\text{FN}_2$; 198.10 (M^+ , Base peak, 100%).

5-(3,5-Dimethoxyphenyl)picolinonitrile (7c) A buff solid; yield = 75%; m.p. = 140–141 °C; R_f = 0.72, EtOAc/petroleum ether (60–80 °C) (1:4). IR (KBr) ν/cm^{-1} : 2965 (sp^3 C–H, stretch), 2227 (CN, stretch), 1602, 1460 (C=N & C=C, stretch). ^1H -NMR; δ 3.83 (s, 6H, *meta*-dimethoxy-H's), 6.62 (s, 1H, Ar–H of dimethoxyphenyl), 6.95 (s, 2H, Ar–H of dimethoxyphenyl), 8.10 (d, J = 7.5 Hz, 1H, Ar–H of picolinonitrile), 8.35 (d, J = 8.1 Hz, 1H, Ar–H of picolinonitrile), 9.10 ppm (s, 1H, Ar–H of picolinonitrile). ^{13}C -NMR; δ 55.48 (2C), 101.24 (1C), 105.43 (2C), 117.65 (1C), 129.01 (1C), 131.32 (1C), 135.61 (1C), 137.25 (1C), 138.86 (1C), 149.48 (1C), 161.13 (2C). MS (EI) (m/e, %) for $\text{C}_{14}\text{H}_{12}\text{N}_2\text{O}_2$; 240.20 (M^+ , Base peak, 100%).

5-(3,5-Dichlorophenyl)picolinonitrile (7d) A white solid; yield = 77%; m.p. = 158–160 °C; R_f = 0.87, EtOAc/petroleum ether (60–80 °C) (1:4). IR (KBr, ν/cm^{-1}): 3078 (sp^2 C–H), 2239 (CN), 1571, 1478, 1426 (C=N & C=C). ^1H -NMR; δ 7.74 (s, 1H, *meta*-dichlorophenyl-H), 7.95 (s, 2H, *meta*-dichlorophenyl-H's), 8.15 (d, J = 8.1 Hz, 1H, Ar–H of picolinonitrile), 8.45 (dd, J = 8.1, 2.4 Hz, 1H, Ar–H of picolinonitrile), 9.16 ppm (s, 1H, Ar–H of picolinonitrile). MS (EI) (m/e, %) for $\text{C}_{12}\text{H}_6\text{Cl}_2\text{N}_2$; 248.10 (M^+ , 59%), 249.05 (12.66%), 251.10 (5.69%); two chlorine isotopes), 99.15 (Base peak, 100%).

General methodology for preparation of picolinamide derivatives 8a–d

The picolinamides **8a–d** were prepared using the same methodology used for formation of monoamides **4a–d**, starting with picolinonitriles **7a–d**.

5-(4-Chlorophenyl)picolinamide hydrochloride salt (8a) A buff solid; yield = 61%; m.p. = 232–234 °C. IR (KBr, ν/cm^{-1}): 3380, 3272 (2NH_2), 3061 (sp^2 C–H), 1688, 1644, 1588 (C=N & C=C). ^1H -NMR; δ 7.62 (d, J = 9 Hz, 2H, Ar–H of *para*-chlorophenyl), 7.92 (d, J = 9 Hz, 2H, Ar–H of *para*-chlorophenyl), 8.44 (d, J = 9 Hz, 1H, Ar–H of picolinamide), 8.50 (d, J = 2.5 Hz, 1H, Ar–H of picolinamide), 9.14 (s, 1H, Ar–H of picolinamide), 9.46 (s, 2H, NH_2 exchangeable with D_2O), 9.66 ppm (s, 2H, $^+\text{NH}_2$ exchangeable with D_2O). ^{13}C -NMR; δ ppm 123.48 (1C), 129.29 (2C), 129.32 (2C), 134.17 (1C), 134.44 (1C), 135.83 (1C), 138.42 (1C), 142.83 (1C), 147.72 (1C), 161.58 (1C). MS (EI) (m/e, %) for $\text{C}_{12}\text{H}_{10}\text{ClN}_3$; 231.00 (M^+ , 10.95), 63.95 (Base peak, 100%).

5-(4-Fluorophenyl)picolinamide hydrochloride salt (8b) A buff solid; yield = 64%; m.p. = 228–230 °C. IR (KBr, ν/cm^{-1}): 3411 (NH), 3052 (sp^2 C–H), 1686, 1596, 1535 (C=N & C=C). ^1H -NMR; δ 7.40 (d, J = 8.5 Hz, 2H, Ar–H of *ortho*-fluorophenyl), 7.96 (d, J = 8.5 Hz, 2H, Ar–H of *meta*-fluorophenyl), 8.46–8.47 (m, 2H, Ar–H of picolinamide), 9.12 (s, 1H, Ar–H of picolinamide), 9.51 (s, 2H, NH_2 exchangeable with D_2O), 9.69 ppm (s, 2H, $^+\text{NH}_2$ exchangeable with D_2O). ^{19}F -NMR ($\text{DMSO}-d_6$); $-\delta$ 112.39 ppm (using TFA as external standard). MS (EI) (m/e, %) for $\text{C}_{12}\text{H}_{10}\text{FN}_3$; 215.05 (M^+ , 24.54%), 199 ($\text{M}^+ + 1 - \text{NH}_3$, Base Peak, 100%).

5-(3',5'-Dimethoxyphenyl)picolinamide hydrochloride salt (8c) A buff solid; yield = 72%; m.p. = 230–232 °C. IR (KBr, ν/cm^{-1}): 3445, 3375 (2NH_2), 3142, 3045 (sp^2 C–H), 2838 (sp^3 C–H), 1689, 1599, 1535 (C=N & C=C). ^1H -NMR; δ 3.83 (s, 6H, *meta*-dimethoxy-H's), 6.63 (s, 1H, Ar–H of dimethoxyphenyl), 6.99 (s, 2H, Ar–H of dimethoxyphenyl), 8.42 (d, J = 8 Hz, 1H, Ar–H of picolinamide), 8.48 (dd, J = 8, 1.5 Hz, 1H, Ar–H of picolinamide), 9.13 (d, J = 1.5 Hz, 1H, Ar–H of picolinamide), 9.45 (s, 2H, NH_2 exchangeable with D_2O), 9.65 ppm (s, 2H, $^+\text{NH}_2$ exchangeable with D_2O). ^{13}C -NMR; δ 55.50 (2C), 101.05 (1C), 105.57 (2C), 123.36 (1C), 136.02 (1C), 137.32 (1C), 139.55 (1C), 142.74 (1C), 147.93 (1C), 161.16 (2C), 161.61 (1C). MS (EI) (m/e, %) for $\text{C}_{14}\text{H}_{15}\text{N}_3\text{O}_2$; 257.10 (M^+ , 39.08), 241.05 ($\text{M}^+ + 1 - \text{NH}_3$, Base peak, 100%).

5-(3',5'-Dichlorophenyl)picolinamidinium hydrochloride salt (8d) A buff solid; yield = 70%; m.p. = 286–288 °C. IR (KBr, ν/cm^{-1}): 3354 (2NH₂), 3053 (sp² C–H), 1690, 1656, 1581 (C=N & C=C). ¹H-NMR; δ 7.76 (s, 1H, Ar–H of 3,5-dichlorophenyl), 8.01 (s, 2H, Ar–H of 3,5-dichlorophenyl), 8.43 (d, $J=8$ Hz, 1H, Ar–H of picolinamidinium), 8.57 (d, $J=8$ Hz, 1H, Ar–H of picolinamidinium), 9.20 (s, 1H, Ar–H of picolinamidinium), 9.45 (s, 2H, NH₂ exchangeable with D₂O), 9.66 ppm (s, 2H, ⁺NH₂ exchangeable with D₂O). ¹³C-NMR; δ 123.37 (1C), 126.26 (2C), 128.71 (1C), 135.03 (1C), 136.54 (2C), 136.90 (1C), 138.88 (1C), 143.56 (1C), 148.12 (1C), 161.43 (1C). MS (EI) (m/e, %) for C₁₂H₉Cl₂N₃; 265.32, 266.94 (M⁺, 5.50; 2.73; two chlorine isotopes), 56.79 (Base peak, 100%).

Toxicity bioassays

Laboratory bioassay

Cotton leaf worm (*S. littoralis*, Family; *Lepidoptera*) Insecticidal efficacy of the newly synthesized compounds against the 2nd instar larvae of *S. littoralis* (Boisd.) was carried out under laboratory conditions. Eggs of *S. littoralis* were acquired from Cotton Leafworm Research Department,

and 800 ppm) were formulated as emulsions in DMF, and 0.1% Triton X-100 was used as a surfactant. The emulsions were freshly used after preparation. For larvicidal achievement, fresh castor bean leaves were dipped in the prepared concentrations of each tested compound for 10 s. The treated leaves were left in the shade to dry before being accessible to the larvae. The larvae were allowed to feed on the treated leaves for 48 h and then changed to untreated leaves. Three replicates of 10 larvae each were used for each concentration in addition to the control. Control (check) tests were carried out using the same technique without the tested compound. Larval mortality counts were calculated for 7 days after the exposure period. Mortality was corrected according to Abbott's formula, and then subjected to probit analysis. The toxicity lines (LC-p lines) were drawn on log concentration–probit paper and statistically analyzed according to Finney's method, to obtain the LC₅₀ and LC₉₀ values of different tested compounds so as to determine the utmost operative one. As well, the efficacy of the examined compounds was assessed by comparing the tested compounds with the most effective compound using the following equation [24, 25]:

$$\text{Toxicity index} = \frac{\text{LC}_{50} \text{ of the utmost effective compound}}{\text{LC}_{50} \text{ of the tested compound}} \times 100$$

Plant Protection Research Institute, Agricultural Research Center, Dokki, Giza, Egypt, and incubated under well-ordered conditions of 25 ± 1 °C and 70 ± 5% RH and kept away from any chemical contamination till the time of treatment to get a susceptible and homogenous strain [24, 25].

Pesticides (*E,Z*)-methyl-*N*-{[(methylamino)carbonyl]oxy}ethanimidothioate which is commercially available under the trade name of lannate 90% soluble powder (SP) (Fig. 3) was purchased from the Central Agricultural Pesticides Laboratory (CAPL) in Dokki, Giza, Egypt.

Toxicological studies The experiments were approved using the leaf dip technique as designated [24, 25]. Six concentrations of each compound (25, 50, 100, 200, 400,

Biochemical aspects Enzymatic activities were assessed in this study using the laboratory strain of 4th instar larvae of *S. littoralis* (Boisd.) after treatment with the tested synthetic biphenyl compounds. At the LC₅₀ value of an aqueous emulsion of each insecticide, castor bean leaves were dipped in for 30 s, then left to dry in shade at r.t for 30 min before being offered to the 4th instar larvae of *S. littoralis*. For 48 h the larvae were nurtured on the treated leaves, and then transferred to feed on freshly untreated leaves for 3 days. From approximately 50 larvae, the haemolymph was attained by removing one of the prolegs with forceps; gentle pressure was applied on the larvae with the fingers and extracting the haemolymph with a syringe. The haemolymph was collected in test tubes and stowed in a refrigerator until the determination of the enzyme's activities [24, 25].

Determination of enzyme activities Alkaline phosphatase (ALK-P) activity was measured according to the reported method [45]. Whereby, acid phosphatase (Acid-p) activity was determined by Fabiny-Byrd & Ertingshausen. Also, the activity of acetylcholine esterase (AChE) was determined according to the described method. The activities of serum esterases including alanine aminotransferase (ALT) and aspartate aminotransferase (AST)

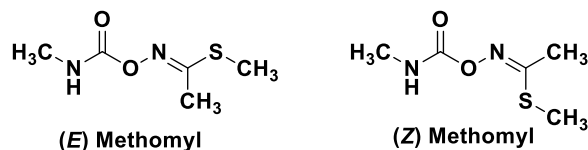


Fig. 3 The chemical structures of recommended, methomyl insecticide, lannate 90% SP

enzymes were estimated calorimetrically. Total proteins were estimated by Bradford's method. Total lipids, lipase, and amylase activities were evaluated according to the reported methods [24, 25].

Statistical analysis

All biological aspects were analyzed using one-way ANOVA by SPSS 13.0 (SPSS, 2004). Duncan's Multiple Range Test (DMRT) was used to determine the probability level to compare the differences among some parameter means ($P < 0.05$) by the Costat system for Windows, Version 6.311, Berkeley, CA, USA, Costat program [46].

Conclusion

In the current work, new two series of halogenated biphenyl and azaphenyl derivatives have been synthesized via the Suzuki coupling reaction. The effect of halogenated azaphenyl substituted on the development of agrochemical fields via investigating their insecticidal activity and plant growth regulators has been studied. In addition, biochemical aspects and enzyme activities were studied. Consequently, the results of this study will provide a new avenue direction for the further structural optimization of halogenated phenyl pyridine analogs as insecticidal. In this study, the calculated chemical quantum descriptors showed excellent agreement with the experimental data displaying that compounds **8d**, **8a**, and **4b** as promising potential candidates against the cotton leafworm, *S. littoralis*.

Supplementary Information

The online version contains supplementary material available at <https://doi.org/10.1186/s13065-023-01050-w>.

Additional file 1. **Figure S1:** IR spectrum of compound 3a. **Figure S2:** ^1H -NMR spectrum of compound 3a. **Figure S3:** Mass spectrum of compound 3a. **Figure S4:** IR Spectrum of compound 3b. **Figure S5:** Mass spectrum of compound 3b. **Figure S6:** ^1H -NMR spectrum of compound 3c. **Figure S7:** Mass spectrum of compound 3c. **Figure S8:** IR spectrum of compound 3d. **Figure S9:** ^1H -NMR spectrum of compound 3d. **Figure S10:** Mass spectrum of compound 3d. **Figure S11:** IR spectrum of compound 4a. **Figure S12:** ^1H -NMR spectrum of compound 4a. **Figure S13:** ^1H -NMR (D_2O) spectrum of compound 4a. **Figure S14:** ^{13}C -NMR spectrum of compound 4a. **Figure S15:** Mass spectrum of compound 4a. **Figure S16:** IR spectrum of compound 4b. **Figure S17:** ^1H -NMR spectrum of compound 4b. **Figure S18:** ^1H -NMR (D_2O) spectrum of compound 4b. **Figure S19:** ^{19}F -NMR spectrum of compound 4b. **Figure S20:** Mass spectrum of compound 4b. **Figure S21:** IR spectrum of compound 4c. **Figure S22:** ^1H -NMR spectrum of compound 4c. **Figure S23:** ^1H -NMR (D_2O) spectrum of compound 4c. **Figure S24:** Mass spectrum of compound 4c. **Figure S25:** IR spectrum of compound 4d. **Figure S26:** ^1H -NMR spectrum of compound 4d. **Figure S27:** ^1H -NMR (D_2O) spectrum of compound 4d. **Figure S28:** Mass spectrum of compound 4d. **Figure S29:** IR spectrum of compound 7a. **Figure S30:** ^1H -NMR spectrum of compound 7a. **Figure S31:** ^{13}C -NMR spectrum of compound 7a. **Figure S32:** Mass spectrum of compound 7a. **Figure S33:** IR spectrum of compound 7b. **Figure S34:** ^1H -NMR spectrum of compound 7b. **Figure S35:** Mass spectrum of compound 7b. **Figure S36:** IR spectrum of compound 7c. **Figure S37:** ^1H -NMR spectrum of compound 7c. **Figure S38:** ^{13}C -NMR spectrum of compound

7c. **Figure S39:** Mass spectrum of compound 7c. **Figure S40:** IR spectrum of compound 7d. **Figure S41:** ^1H -NMR spectrum of compound 7d. **Figure S42:** Mass spectrum of compound 7d. **Figure S43:** IR spectrum of compound 8a. **Figure S44:** ^1H -NMR spectrum of compound 8a. **Figure S45:** ^1H -NMR (D_2O) spectrum of compound 8a. **Figure S46:** ^{13}C -NMR spectrum of compound 8a. **Figure S47:** Mass spectrum of compound 8a. **Figure S48:** IR spectrum compound 8b. **Figure S49:** ^1H -NMR spectrum of compound 8b. **Figure S50:** ^1H -NMR (D_2O) spectrum of compound 8b. **Figure S51:** ^{19}F -NMR spectrum of compound 8b. **Figure S52:** Mass spectrum of compound 8b. **Figure S53:** IR spectrum of compound 8c. **Figure S54:** ^1H -NMR spectrum of compound 8c. **Figure S55:** ^1H -NMR spectrum of (D_2O) compound 8c. **Figure S56:** ^{13}C -NMR spectrum of compound 8c. **Figure S57:** Mass spectrum of compound 8c. **Figure S58:** IR spectrum of compound 8d. **Figure S59:** ^1H -NMR spectrum of compound 8d. **Figure S60:** ^1H -NMR (D_2O) spectrum of compound 8d. **Figure S61:** The ^{13}C -NMR spectrum of compound 8d. **Figure S62:** Mass spectrum of compound 8d.

Acknowledgements

The authors are indebted to Mansoura University for all support and the facilities provided.

Author contributions

EG: conceptualization, methodology of organic synthesis, software, investigation, writing—original draft. HA: methodology of organic synthesis, formal analysis. ML: Conceptualization, Formal analysis, supervision and editing review and AF: supervision. MS conceptualization, software, investigation, biological aspects experiments data, writing—original draft. All authors reviewed the manuscript.

Funding

Open access funding provided by The Science, Technology & Innovation Funding Authority (STDF) in cooperation with The Egyptian Knowledge Bank (EKB).

Availability of data and materials

All data and analysis during this study are available in this article and its Additional file 1.

Declarations

Ethics approval and consent to participate

All experiments and methods were performed in accordance with relevant guidelines approved by the Committee of Research Ethics in Mansoura University, Egypt with code MU-ACUC (Sc. MS. 23.04.21).

Consent for publication

Not applicable.

Competing interests

The authors declare that they have no competing interests.

Author details

¹Present Address: Chemistry Department, Faculty of Science, Mansoura University, Mansoura 35516, Egypt. ²Plant Protection Research Institute, ARC, Dokki, Giza, Egypt.

Received: 3 June 2023 Accepted: 29 September 2023

Published online: 27 October 2023

References

- Xu FZ, Wang YY, Luo DX, Yu G, Guo SX, Fu H, Zhao YH, Wu J. Design, synthesis, insecticidal activity and 3D-QSR study for novel trifluoromethyl pyridine derivatives containing an 1,3,4-oxadiazole moiety. *RSC Adv*. 2018;8:6306–14.

2. Bajsa N, Fabiano E, Rivas-Franco F. Biological control of phytopathogens and insect pests in agriculture: an overview of 25 years of research in Uruguay. *Environ Sustain*. 2023;6:121–33.
3. Kamel MS, Aboelez MO, Elnagar MR, Shokr EK, Selim HMRM, Abdel-Ghany HE, Drar AM, Belal A, El Hamd MA, El-Remaily MAEAAA. Green synthesis design, spectroscopic characterizations, and biological activities of novel pyrrole derivatives: an application to evaluate their toxic effect on cotton aphids. *ChemistrySelect*. 2022;7(40):e202203191.
4. Fanzo J, Rudie C, Sigman I, Grinspoon S, Benton TG, Brown ME, Covic N, Fitch K, Golden CD, Grace D, Hivert M-F, Huybers P, Jaacks LM, Masters WA, Nisbett N, Richardson RA, Singleton CR, Webb P, Willett WC. Sustainable food systems and nutrition in the 21st century: a report from the 22nd annual Harvard Nutrition Obesity Symposium. *Am J Clin Nutr*. 2022;115(1):18–33.
5. Serraj R, Krishnan L, Pingali P. Agriculture & food systems to 2050. In: Serraj R, Pingali P, editors. *Global trends, challenges and opportunities*. Italy: Food and Agriculture Organization of the United Nations; 2018.
6. Alves J, Gaspar PD, Lima TM, Silva PD. What is the role of active packaging in the future of food sustainability? A systematic review. *J Sci Food Agric*. 2023;103(3):1004–20.
7. Zhang W, Chen J, Du X. 2-Phenylpyridine derivatives: synthesis and insecticidal activity against *Mythimna separata*, *Aphis craccivora*, and *Tetranychus cinnabarinus*. *Molecules*. 2023;28(4):1567.
8. Guo Y. Soil fungi and the insect gut microbiota. *Nature Food*. 2023;4(3):200.
9. Abdelhamid AA, Salama KSM, Elsayed AM, Gad MA, El-Remaily MAEAAA. Synthesis and Toxicological effect of some new pyrrole derivatives as prospective insecticidal agents against the cotton leafworm, *Spodoptera littoralis* (Boisduval). *ACS Omega*. 2022;7(5):3990–4000.
10. Eroglu GB. *Pest insects and their biological control*. 1st ed. London: IntechOpen; 2022.
11. Elmenofy W, Salem R, Osman E, Yasser N, Abdelmawgod A, Saleh M, Aya Z, Hanafy E, Tamim S, Amin S, El-Bakry A, El-Sayed A, El-Gaied L. Evaluation of two viral isolates as a potential biocontrol agent against the Egyptian cotton leafworm, *Spodoptera littoralis* (Boisd.) (Lepidoptera: Noctuidae). *Egypt J Biol Pest Control*. 2020;30:1–8.
12. El-Husseini MM, El-Heneidy AH, Awadallah KT. Natural enemies associated with some economic pests in Egyptian agro-ecosystems. *Egypt J Biol Pest Control*. 2018;28(1):1–17.
13. Elhady OM, Mansour ES, Elwassim MM, Zawam SA, Drar AM. Synthesis and characterization of some new tebufenozide analogues and study their toxicological effect against *Spodoptera littoralis* (Boisd.). *Curr Chem Lett*. 2022;11(1):63–8.
14. Khodairy A, Mansour ES, Elhady OM, Drar AM. Novel *N*-cyanoguanidyl derivatives: synthesis and studying their toxicological activity against *Spodoptera littoralis* and *Schizaphis graminum*. *Curr Chem Lett*. 2021;10(4):363–70.
15. Bazazo KGI. The role of cotton leafworms control with certain insecticides in increasing sugar beet crop productivity. *Zagazig J Agric Res*. 2019;46(6):2229–38.
16. Ahmed K, Mikhail WZA, Sobhy HM, Radwan EMM, El Din TS, Youssef A. Effect of lambda-cyhalothrin as nanopesticide on cotton leafworm, *Spodoptera littoralis* (Boisd.). *Egypt J Chem*. 2019;62(7):1263–75.
17. Khodery A, Mansour ES, Elhady OM, Drar AM. Synthesis of Neonicotinoid analogues and study their toxicological aspects on *Spodoptera littoralis* and *Schizaphis graminum*. *Int J Pest Manag*. 2021. <https://doi.org/10.1080/09670874.2021.1943048>.
18. Aktar MW, Sengupta D, Chowdhury A. Impact of pesticides use in agriculture: their benefits and hazards. *Interdiscip Toxicol*. 2009;2(1):1–12.
19. Tudi M, Ruan HD, Wang L, Lyu J, Sadler R, Connell D, Chu C, Phung DT. Agriculture development, pesticide application and its impact on the environment. *Int J Environ Res Public Health*. 2021;18(3):1112.
20. Gyawali K. Pesticide uses and its effects on public health and environment. *J Heal Promot*. 2018;6:28–36.
21. El-Dean AMK, Abd-Ella AA, Hassanien R, El-Sayed MEA, Abdel-Raheem SAA. Design, synthesis, characterization, and insecticidal bioefficacy screening of some new pyridine derivatives. *ACS Omega*. 2019;4(5):8406–12.
22. Cai Z, Zhang W, Cao Y, Du X. Synthesis and herbicidal activities of 2-phenylpyridine compounds containing alkenyl moieties. *J Heterocycl Chem*. 2022;59(7):1247–52.
23. Rashid KO, Mohamed KS, Abd El Salam M, Abdel-Latif E, Fadda AA, Elmorsy MR. Synthesis of novel phenoxyacetamide derivatives as potential insecticidal agents against the cotton leafworm, *Spodoptera littoralis*. *Polycycl Aromat Compd*. 2023;43(1):356–69.
24. Soliman NN, Abd El Salam M, Fadda AA, Abdel-Motaal M. Synthesis, characterization, and biochemical impacts of some new bioactive sulfonamide thiazole derivatives as potential insecticidal agents against the cotton leafworm, *Spodoptera littoralis*. *J Agric Food Chem*. 2020;68(21):5790–805.
25. Fadda AA, Abd El Salam M, Tawfik EH, Anwar EM, Etman HA. Synthesis and insecticidal assessment of some innovative heterocycles incorporating a thiadiazole moiety against the cotton leafworm, *Spodoptera littoralis*. *RSC Adv*. 2017;7:39773–85.
26. El-Gaby MSA, Hussein MF, Faraghal FA, Drar AM, Gad MA. Insecticidal activity and structure activity relationship study of some synthesized hydrazone, dihydropyridine and 3-cyano-1,4-dihydro-pyrazidin-4-one derivatives against *Aphis nerii*. *Curr Chem Lett*. 2023;12(3):599–606.
27. Jeschke P. Manufacturing approaches of new halogenated agrochemicals. *Eur J Org Chem*. 2022;12:e202101513.
28. Ogawa Y, Tokunaga E, Kobayashi O, Hirai K, Shibata N. Current contributions of organofluorine compounds to the agrochemical industry. *Iscience*. 2020;23(9):101467.
29. Ali HA, Ismail MA, Fouda AE-AS, Ghaith EA. A fruitful century for the scalable synthesis and reactions of biphenyl derivatives: applications and biological aspects. *RSC Adv*. 2023;13:18262–305.
30. Edelmann FT. Recent progress in the chemistry of metal amidinates and guanidinates: syntheses, catalysis and materials. *Adv Organomet Chem*. 2013;61:55–374.
31. Boeré RT, Oakley RT, Reed RW. Preparation of *N, N, N'*-tris (trimethylsilyl) amidines; a convenient route to unsubstituted amidines. *J Organomet Chem*. 1987;331(2):161–7.
32. Ghazy NM, Ghaith EA, Abou El-Reash YG, Zaky RR, Abou El-Maaty WM, Awad FS. Enhanced performance of hydroxyl and cyano group functionalized graphitic carbon nitride for efficient removal of crystal violet and methylene blue from wastewater. *RSC Adv*. 2022;12:35587–97.
33. Abdallah AB, Ghaith EA, Mortada WI, Molouk AFS. Electrochemical sensing of sodium dehydroacetate in preserved strawberries based on in situ pyrrole electropolymerization at modified carbon paste electrodes. *Food Chem*. 2023;401:134058.
34. Hamama WS, Ghaith EA, Ibrahim ME, Sawamura M, Zoorob HH. Synthesis of 4-hydroxy-2-pyridinone derivatives and evaluation of their antioxidant/anticancer activities. *ChemistrySelect*. 2021;6(7):1430–9.
35. Ghaith EA, Zoorob HH, Ibrahim ME, Sawamura M, Hamama WS. Convenient synthesis of binary and fused pyrazole ring systems: accredited by molecular modeling and biological evaluation. *ChemistrySelect*. 2020;5(47):14917–23.
36. Sayin K, Karakaş D. Investigation of structural, electronic and biological properties of two Zn (II) complexes with pentaaza macrocyclic schiff-base ligand: a DFT approach. *J Cluster Sci*. 2017;28:3075–86.
37. Parthasarathi R, Subramanian V, Roy DR, Chattaraj PK. Electrophilicity index as a possible descriptor of biological activity. *Bioorg Med Chem*. 2004;12(21):5533–43.
38. Wu J, Kang S, Yuan Q, Luo L, Ma J, Shi Q, Yang S. *N*-substituted 5-chloro-6-phenylpyridazin-3(2H)-ones: synthesis, insecticidal activity against *Plutella xylostella* (L.) and SAR study. *Molecules*. 2012;17(8):9413–20.
39. Ismail MA, Abdel-Rhman MH, Abdelwahab GA, Hamama WS, El-Shafeai HM, El-Sayed WM. Synthesis of new thienylpicolinamide derivatives and possible mechanisms of antiproliferative activity. *RSC Adv*. 2020;10:41165–76.
40. Liao Y, Yang W, Wei T, Cai M. A highly efficient and recyclable NiCl₂(dppp)/PEG-400 system for Suzuki-Miyaura reaction of aryl chlorides with arylboronic acids. *Synth Commun*. 2019;49(9):1134–42.
41. Wang F, Wang C, Sun G, Zou G. Highly efficient palladium-catalyzed cross-coupling of diarylboronic acids with arenediazoniums for practical diaryl synthesis. *Tetrahedron Lett*. 2020;61(7):151491.
42. Mashweu AR, Chhiba-Govindjee VP, Bode ML, Brady D. Substrate profiling of the cobalt nitrile hydratase from *Rhodococcus rhodochrous* ATCC BAA 870. *Molecules*. 2020;25(1):238.
43. Greig IR, Baillie GL, Abdelrahman M, Trembleau L, Ross RA. Development of indole sulfonamides as cannabinoid receptor negative allosteric modulators. *Bioorg Med Chem Lett*. 2016;26(18):4403–7.

44. Sinha S, Ahire D, Wagh S, Mullick D, Sistla R, Selvakumar K, Cortes JC, Putlur SP, Mandekar S, Johnson BM. Electrophilicity of pyridazine-3-carbonitrile, pyrimidine-2-carbonitrile, and pyridine-carbonitrile derivatives: a chemical model to describe the formation of thiazoline derivatives in human liver microsomes. *Chem Res Toxicol*. 2014;27:2052–61.
45. Sharma S, Gupta N, Chakkal AS, Sharma N, Alamri S, Siddiqui MH, Haider FU. Changes in enzyme activities in salt-affected soils during incubation study of diverse particle sizes of rice straw. *Agriculture*. 2023;13(9):1694.
46. Costat Program. Version 6.311. Monterey: Cohort Software Inc.; 2006.

Publisher's Note

Springer Nature remains neutral with regard to jurisdictional claims in published maps and institutional affiliations.

Ready to submit your research? Choose BMC and benefit from:

- fast, convenient online submission
- thorough peer review by experienced researchers in your field
- rapid publication on acceptance
- support for research data, including large and complex data types
- gold Open Access which fosters wider collaboration and increased citations
- maximum visibility for your research: over 100M website views per year

At BMC, research is always in progress.

Learn more biomedcentral.com/submissions

